

Beam-beam collision monitoring for CESR: A Large Angle Beamstrahlung Monitor

1 Introduction

The development of high-luminosity e^+e^- colliders has been a major focus of the High Energy Physics (HEP) community over the last decade. This proposal describes a technique, large angle beamstrahlung (developed mainly by our group over the last three years [1 – 5]), and instrument that gives much more information than present luminosity monitors about the beam-beam collision region of such colliders. It offers the opportunity to increase the integrated luminosity by a factor which is difficult to quantify but ranges from 10 to 50% at a very modest cost. We intend to build and install the monitor at the Cornell Electron Storage Ring (CESR), funded by the National Science Foundation, develop the techniques of collision region monitoring, and quantify the gain in integrated luminosity.

Our group is uniquely qualified for this project. Prof. Bonvicini has had a long-term involvement with beamstrahlung, as shown by his publication list and references at the end of this proposal. Prof. Cinabro is the current CLEO spokesperson in part due to his many contributions to machine issues[6]. In the last three years, he has developed a technique, similar to Positron Emission Tomography in medicine, which measures directly the properties of the beams at the collision point[7 – 8] by measuring the density of event vertices and angular distributions of two lepton events using the CLEO detector. The latter technique is, at present, limited to offline studies of CESR, and only for runs which have well-understood beam optics. It is developed and will continue to be developed together with the technique described here, and will provide cross-checks that no other technique could provide.

Our international collaborators are just as qualified. Prof. Coisson of University of Parma initiated the whole field with a seminal 1979 paper, in which he extracted the generalized form for large angle synchrotron radiation [9] and found it to be vastly different from “classical” synchrotron radiation formulae. He measured first the properties of such radiation[10], wrote the first, very important, paper that discusses large angle beamstrahlung[11] (which, in turn, inspired the first experimental proposal [12]) and for twenty years has continued to work on synchrotron radiation while proposing the various forms of synchrotron radiation as powerful beam monitors[13 – 14]. Prof. Patel of McGill University is a current CLEO member and future BABAR collaborator. He has worked previously at the interface between machine and detector[15], and has an interest in developing the technique for future applications, in particular BABAR.

There are seven transverse degrees of freedom (*dof*) in a beam-beam collision as shown in Figure 1. Typically beams are made to overlap at the beginning of a machine run, after which they start to drift independently in shape, size, location and orientation. The drifts are generated by the continuous, small, and random changes of many machine components such as the beam currents and magnet strengths. Due to the beam sizes a drift of 10 microns, a rotation of 2 degrees, or a bloating of 10 microns by one beam at any of the *B*-factories is enough to spoil the luminosity. Even a symmetric *B*-factory such as CESR suffers from differences between the two beams at the collision region due to differences in

the machine lattice for electrons and positrons, the so-called “pretzel” scheme, and coupling introduced by the CLEO solenoid and magnet non-linearities. As a result beams may collide asymmetrically (three of the four non-optimal beam-beam collisions shown in Fig. 2 are readily observed at CESR), decreasing the luminosity delivered to the CLEO experiment.

The enclosed letters of support, from the director of the Cornell Electron Storage Ring and the director of PEP-II at the Stanford Linear Accelerator Center, describe the enormous problems encountered in trying to maintain beam-beam overlap against the hundreds of drifting components around the machine. The detector developed in this proposal identifies the problem, identifies which beam needs to be corrected, and by how much it needs to be corrected, regardless of the source of the problem[2]. An iterative procedure allows to do the same if the problem is a combination of two or more effects, such as bloating and rotation at the same time[2].

A bibliographic search using the title keyword “beam-beam” produces 545 papers over the last 20 years. By providing this much information, this device will help settle what has been a long-standing technical problem in accelerator physics, with attendant benefits in improved physics outputs. A major issue is the tune-shift limit, which for flat beams is roughly 0.06. Extensive studies of its validity and its scaling properties have never been undertaken, but they will become possible if substantially new, instantaneous information on the beam-beam collision becomes available. Even the measurement of longitudinal degrees of freedom, such as the beam length, become possible[1].

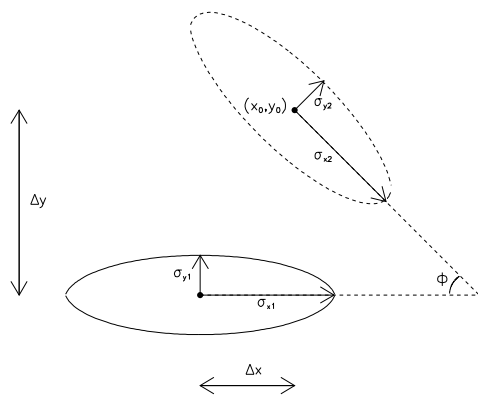


Figure 1: A general beam-beam collision. Seven parameters can be seen, corresponding to two transverse dimensions for each beam, a two dimensional impact parameter vector connecting the two beam centers, and one relative rotation in the transverse plane.

The beamstrahlung monitor would improve on *existing* beam-beam monitoring methods. Currently the beam properties at the collision point are monitored in two ways. In one

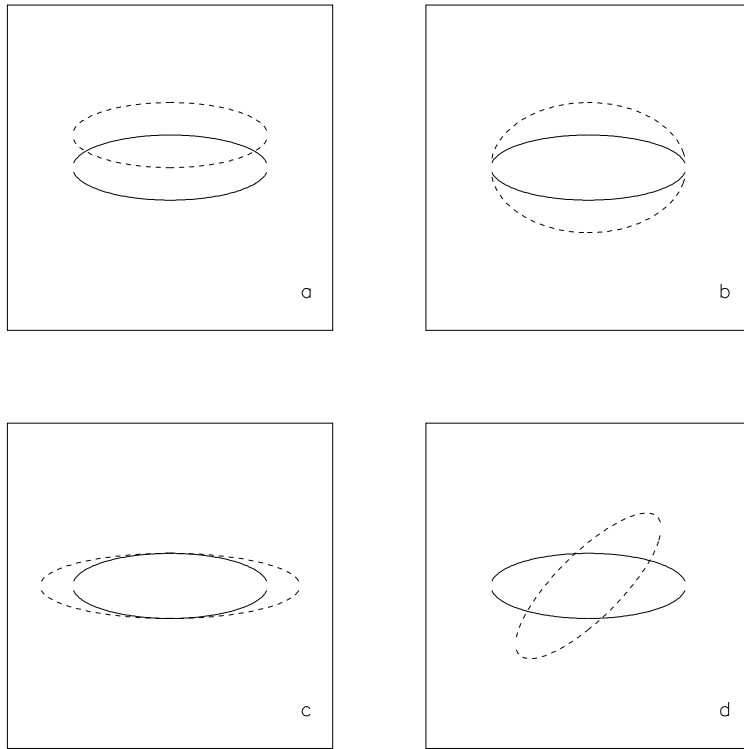


Figure 2: The four beam-beam pathologies that lead to wasted luminosity; a) a y - offset; b) y - bloating; c) x - bloating; and d) a beam-beam rotation. The pathological beam is represented by the dashed ellipse.

method, the beams are artificially displaced and their deflection is measured [16 – 17]. This method is direct, but really only measures one of the seven *dof*, the beam width along the displacement’s direction. Measurements are also made of orbital parameters at other locations in the machine, and their values are related to the beam parameters at the collision points. The accuracy of this method depends on the knowledge of the instantaneous Twiss matrix of the machine. This is known only to a certain extent, making the method unreliable.

Beamstrahlung is the electromagnetic radiation emitted by one beam as its particles are bent by the electromagnetic field of the opposing beam. By observing the light produced at large azimuthal angles and the polarizations corresponding to the machine transverse axes, six of the seven transverse degrees of freedom can be effectively monitored[2]. The one *dof* which can not be measured by beamstrahlung is the vertical beam width, which is the only one which is already measured directly [16].

The beamstrahlung detector is conceptually fairly simple, but we found in extensive simu-

lations that large synchrotron radiation backgrounds from the Interaction Region quadrupoles force two changes from a minimal design. First, we need to work at infrared wavelengths, while preserving fast-timing. We need to use photomultipliers which are sensitive to infrared radiation. Second, discrimination against backgrounds comes predominantly from large angle observation. High quality optics and alignment are needed.

The development into a feedback device is not trivial and very labor intensive. This explains the need for a dedicated postdoc, as well as our collaborative effort. The technique is meant to reduce an enormously complex problem to a small set of feedback algorithms. Proper interfacing with the machine feedback system, on-line data analysis, including background determination and subtraction, corrections for changing beam current and beam angle, off-line data analysis, and on-line graphical user interfaces all need to be developed. The beamstrahlung data and CLEO detector data, which monitors the luminosity and the horizontal beam size [7], belong to two completely independent data streams, which need to be brought into the same computing environment.

High-energy beamstrahlung has already been used as a main beam-beam monitor for the Stanford Linear Collider[18–19]. That monitor had a much more limited scope than the one proposed here. While very useful, it provided little more than the measurement of the total beamstrahlung power emitted by either beam. This proposal aims at beam-beam pattern recognition, for which polarization information is necessary.

If this proposal is successful, a novel, very powerful technique will be established and its future will be bright. Not only will it be able to substantially increase the luminosity output of prime national and international facilities, it could play a pivotal role in future linear colliders, which cost several billion dollars and appear to be the next major high energy physics project. At linear colliders, beams of size tens of nanometers across are aimed at one another from distances of tens of kilometers and must be kept in collision for extended periods of time. No method has been proposed to measure *directly* the pattern of the beam-beam collision with such microscopic beams. In Ref.[4], one of our students designed a beamstrahlung detection method which can collect the entire beamstrahlung signal at the NLC while suppressing backgrounds by at least four orders of magnitude.

2 Results from prior NSF support.

Our group has a research grant from NSF, PHY-9804607, for research in HEP at CLEO. Besides our HEP work we have led the effort to build the CLEO III Interaction Region (IR). Much of the design work was done by Professor Cinabro, and he led a construction and assembly team from Wayne State, Cornell, and external vendors. Professor Cinabro has worked on optimizing the CESR machine for nearly ten years [6] and has pioneered the techniques of monitoring the CESR collision region with the CLEO detector[7]. Professor Cinabro is currently the co-spokesperson of the CLEO Collaboration. Professor Bonvicini has led our effort on wide angle beamstrahlung. We have not received MRI support previously.

We have also run a very successful REU program, NSF grant PHY-9820306, in collaboration with Cornell's Laboratory of Nuclear Studies[20]. Two of the REU students have worked with us on the beamstrahlung project, both at Cornell and in the following Fall.

3 Research Activities.

The conceptual design of the large angle beamstrahlung detector is complete [5]. The next stage is the engineering design and the construction of the beamstrahlung detector. A variety of issues needs to be addressed, including machine and vacuum compatibility, thermal and alignment problems, precision optics, photomultiplier characterization, and assembly. Fast-gating and data acquisition electronics need to be acquired and made operational. Finally, the beamstrahlung data need to be interfaced with the CESR control system.

The beamstrahlung monitor will need an extensive testing period to quantify its use. In machine development it can be used by accelerator physicists in studies of the beam-beam limit and its scaling properties, measurement of the beam length, measurement of the beam transverse dimensions, and measurement of bunch-dependent effects. For this purpose the detector should be “turn key” system. For on line monitoring during HEP running for CLEO the detector has to measure drifts in transverse space and automatically correct them.

The device will provide several graduate theses. Two Wayne State undergraduates (E. Luckwald and N. Detgen) have already been co-authors beamstrahlung-related papers[2, 5]. We can anticipate that beamstrahlung data will be heavily used by the CESR Machine Group, which consists of some 20 senior physicists, looking for various effects, some of which might not be included in the list above. Their usage pattern will ultimately quantify the success of the project.

The ultimate output of the beamstrahlung monitor is, of course, used by the 220 physicists of the CLEO Collaboration in the form of a higher integrated luminosity.

After commissioning, much of the study will be carried out using the “beamstrahlung diagram” [2], which is a simple and exact graphic device by which a two-arrow configuration, one for each beam, is plotted using the beamstrahlung data. Each arrow has x - and y - components proportional to the polarized light yield along those transverse axes. The diagrams corresponding to the four “pathologies” shown in Figure 2 are shown in Figure 3. In Reference [2] a quantitative relation is established between the diagrams and the beam-optics correction to be applied. For example in Fig. 3a) the distance of the vectors from 45 degrees line is a measure of the y -offset, and in Fig. 3d) the arc between the equal vectors is a measure of relative rotation. The correction is unambiguously determined, the beam that needs correction is determined (always the one with the highest y polarization), and the amount of the correction is also measured [2]. Further, by measuring the evolution of the diagram after the first correction, a six-dimensional space can be effectively monitored by the 4-dimensional diagram.

4 Research Instrumentation and needs.

The “beamstrahlung diagram” requires that both x and y polarized powers on each side of the Interaction Point (IP), East and West, be monitored. In fact, both beams can (and do) rotate away from their nominal orientation, making a third measurement necessary. We choose to have a fourth measurement for background control.

Any photosensitive device looking inside an electron storage ring is bound to see a lot of light. Background rejection is the dominant experimental issue in this project. In view of

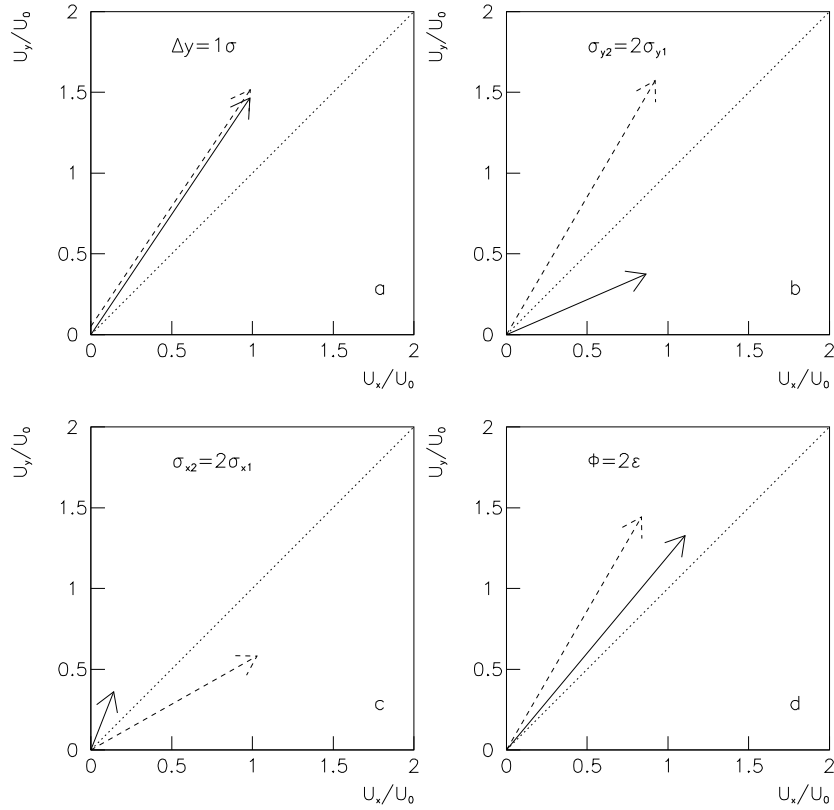


Figure 3: Beamstrahlung diagrams corresponding to the four pathologies of Figure 2. The tips of vectors in part a) are displaced for display purposes.

the pioneering nature of our proposal, we chose to give as detailed as possible a presentation of the backgrounds and of the ways to deal with them.

At CESR Phase III, 7W of beamstrahlung power is produced, which is dwarfed by the various sources of synchrotron background near the IR. The accelerator environment provides substantial constraints. Breaking the CESR vacuum more than once would cost more than the beamstrahlung monitor itself, and it is shown below that even the simplest possible preliminary measurement would entail the construction of a substantial optical system, which would in turn cost as much as half this proposal.

There is much in common between this project and the previous beamstrahlung monitor at the SLC:

- most of the funds need to be spent up front, involving a certain risk. At the SLC, the bulk of the funds went into substituting the two large hard-bend magnets with new,

large-aperture magnets that could allow beamstrahlung to get to the detectors.

- several of the background sources had not been directly measured. One relies on careful simulations and large safety factors.
- several potential background sources are common to the SLC, and we draw on that experience to quantify them.

At the SLC backgrounds at the primary mirror were about one million times higher than the signal (in total power). In our initial investigation, we found one overwhelming background (Cherenkov light in the photomultipliers photocathodes) which necessitated a careful simulation and ultimately a major design change. For this, the detector was designed with a few orders of magnitude safety cushion with respect to this background. We also found one possibly substantial (scintillation in the Cherenkov counter gas) background, which was dealt with by carefully choosing the Cherenkov gas, and limiting the solid angle. All other backgrounds (mirror fluorescence, Thompson scattering) were judged to be negligible and turned out to be so.

At CESR we found an overwhelming source of background (quadrupole synchrotron radiation) that necessitated major changes in design, and we gave ourselves several orders of magnitude as a safety cushion, Fig. 5. We found one potentially substantial source of background (rescattered radiation), which is dealt with by reducing the solid angle and placing the detectors in a sheltered location, Fig. 4. All other backgrounds are almost certainly negligible.

At the SLC, a beamstrahlung signal was obtained[18] by exploiting the difference between the beam magnetic field (10-100 T) and the other magnetic fields along the beam line (0.1-1 T). The larger magnetic fields resulted in a higher cutoff energy for beamstrahlung, and a favorable signal/noise could be obtained for photons of approximately 20 MeV energy. At CESR, the magnetic field of the beams and of the magnets along the beam line have the same order of magnitude (0.1-1 T), eliminating this possibility. The wider angular spread of beamstrahlung radiation, compared to normal synchrotron radiation, is used instead.

The large-angle power emitted as a function of angle and frequency is expressed as [11]

$$I(\theta, \phi, \omega) = \frac{3\sigma_z W_1}{4\pi\sqrt{\pi}c} \frac{1}{\gamma^4 \theta^3} \exp\left(\frac{-\sigma_z^2 \theta^4 \omega^2}{16c^2}\right). \quad (1)$$

The exponential factor in Equation 1 is of fundamental importance for this project. An exponential dependence on the magnet length is always present at large angle, in a deviation from the “classical” synchrotron radiation equations[3]. CESR magnets are typically one hundred times longer than the beams, resulting in a much more collimated synchrotron beam, and a favorable signal/noise ratio can be obtained at a large enough angle and a large enough wavelength.

Eq.(1) summarizes the needs of a large angle beamstrahlung monitor. The detector must work at a large enough angle that normal synchrotron radiation is suppressed, at a wavelength such that enough signal is available. Sharp angular acceptance is the only tool to avoid the overwhelming synchrotron backgrounds.

We choose for our detector a location at 5.6 meters from the IP, which has been allocated to our project. Here the beam pipe is round and has an inner radius of 6.36cm. Assuming

a rectangular primary mirror with the outer edge at the beam pipe, with a solid angle acceptance of $(1\text{mrad})^2$, the inner edge is located at 5.72 cm, 1.58 cm outside the stay clear envelope. The beam pipe becomes elliptical nearby, a fact that helps substantially in background reduction (Fig. 4), as explained below.

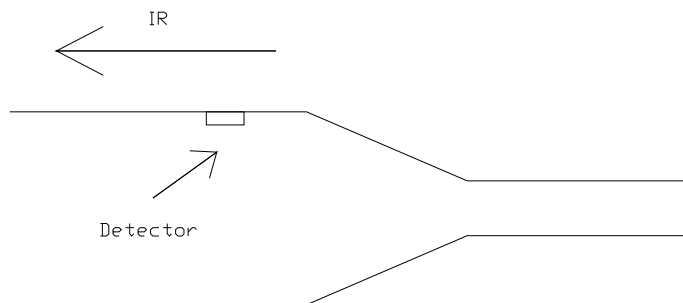


Figure 4: Beam pipe profile near the beamstrahlung detector location. The IP is located to the left of the funnel. The beamstrahlung detector is located to the left of the funnel, at 5.6 meters from the IP. The funnel itself is located between 6.00 and 6.22 meters from the IP.

The detector design is then dictated by the need to suppress the backgrounds. The beam-beam collision rate is 17MHz, and even a very modest signal will result in a large statistics over one second. The dominant source of synchrotron radiation striking the primary mirrors are the final focusing superconducting quadrupoles around the IP. Detector feasibility depends almost solely on shielding against this source of backgrounds. The next subsection discusses our simulation, which is described in more detail in Ref.[5].

4.1 Quadrupole synchrotron radiation.

In Ref.[1] it was computed that for a parallel beam a location beyond 6 milliradians would experience negligible synchrotron backgrounds. The large angular divergence of the beam at certain locations in the quadrupoles generates a radiation spray which spreads out much more than 6 milliradians. The quadrupole radiation was the object of a careful simulation. It was relevant to simulate synchrotron radiation properly[3], so a new algorithm was developed, and also to test “real life” changes in the machine. The beam line and beam optics used were the nominal CESR Phase III conditions, but the beam position and angle were varied, both in x (the horizontal component) and in y (vertical), within the CESR tolerances.

“Detectors” (1 milliradian square holes) were placed at every ten degrees in azimuth with respect to the x - axis, starting at 30 degrees, and the power striking the detector was computed (both total and in the infrared window of interest). The 30 degree location is the outermost one, and the 150 degrees the innermost one with respect to the CESR ring. The typical total power striking the mirrors varies from 0.1pW at 60 degrees to $10\mu\text{W}$ at 150 degrees. After identifying the 60 degrees region as the optimal one, the final choice of azimuth for the two detectors were 50 and 72.5 degrees (the beamstrahlung radiation has an

eight-fold pattern, replicating itself every 45 degrees [1,2,11]. The counters are optimally separated by an odd number of 22.5 degrees arcs).

The beam was simulated out to 10σ in both x and y , and was step-transported across the quadrupoles. At each step, the angle between electron and detector, and the bending force were computed. Using prepared lookup tables, the power to each detector location, were calculated and summed. The beams enter and exit the IP at an angle in the $x - z$ plane, pointing inward with respect to CESR, and for each simulation the 150 degrees counter had the smallest effective angle with respect to the beam direction, and the 30 degrees counter the largest.

The synchrotron backgrounds were computed according to the methods described in Ref. [3]. Briefly, the radiation could be distributed according to the classical “searchlight” approximation[21], or according to Coisson’s “short magnet” approximation[9]. These approximations are extreme: the former assumes that the electron is sweeping in its bending plane, effectively covering all angles above a minimum, the second assumes that the angle between detector and electron remains fixed. The two approximation differ by many orders of magnitude at certain locations in angle and frequency (while predicting the same power, the same average angle, and the same average polarization). We found that the two approximations yielded the same results (to within 20%) when convoluted over the quadrupoles beam envelope. The short magnet approximation yielded always the largest backgrounds, particularly in the infrared region, and was used to produce the plots shown below.

By plotting various quantities we learned that backgrounds come mostly from well-defined, small regions within the quadrupoles, where the particle’s angle with respect to the axis is maximal, and two to seven standard deviations away from the center. The particles producing the most background are those pointing in the general direction of the counter, and the background is 90% radially polarized, a fact we could have used for background reduction but deemed unnecessary.

When studying the signal/noise ratio, we tried to implement the “magic angle” strategy of Ref. [1]. Given the wavelength at which one wants to observe beamstrahlung (“red”), the detector is placed at the angle at which the exponent in Eq.1 is equal to -2. At half the wavelength (“blue”), the exponent will be equal to -8 and a measure of the “blue” will measure backgrounds, while the “red” measures both signal and background. We hoped that we could work with real red ($\lambda = 660\text{nm}$) and blue ($\lambda = 330\text{nm}$) light using standard, cheap photomultipliers, but the synchrotron radiation background generated by the incoming beam in the final focus quads were of the same order of the signal. Following Reference [1], we moved to higher wavelengths. We still use visible light (as seen by standard photomultipliers) as the background control sample.

In the near infrared ($0.9 < \lambda < 1.0\mu\text{m}$) a favorable signal/background was obtained. Table 1 shows the total power striking the mirrors, and the power within the angular acceptance of the optical acceptance, for each of the five counters, for various beam parameters and for also different optics. Nominal conditions were assumed to be: $x_{IP} = -2\text{mm}$, $x'_{IP} = -2.2\text{mrad}$, $\sigma_z = 18\text{ mm}$, and $I_{beam} = 0.5\text{ A}$. y_{IP} and y'_{IP} were kept equal to zero except for a series of simulation were a positive and negative $1\text{mrad } y$ -bump was simulated. A different lattice was also tried for the purpose of assessing the impact of changing the optics on the background. Other beam parameters relevant for the beamstrahlung signal are $\sigma_x = 450\mu\text{m}$, $\sigma_y = 10\mu\text{m}$, and $f = 17\text{MHz}$.

Collision conditions (mm,mrad)	Counter Azimuth	$W_{rad.}(W)$	$W_{tan.}(W)$
Nominal(see text)	30	2×10^{-32}	1×10^{-33}
Nominal	60	4×10^{-24}	3×10^{-25}
Nominal	90	1×10^{-9}	9×10^{-11}
Nominal	120	2×10^{-11}	2×10^{-12}
Nominal	150	4×10^{-26}	5×10^{-27}
$x_{IP} = -2.2, x'_{IP} = -3$	30	9×10^{-25}	5×10^{-26}
$x_{IP} = -2.2, x'_{IP} = -3$	60	1×10^{-17}	1×10^{-18}
$x_{IP} = -2.2, x'_{IP} = -3$	90	1×10^{-11}	1×10^{-12}
$x_{IP} = -2.2, x'_{IP} = -3$	120	2×10^{-8}	2×10^{-9}
$x_{IP} = -2.2, x'_{IP} = -3$	150	2×10^{-8}	2×10^{-9}
$x_{IP} = 0, x'_{IP} = -1.5$	30	9×10^{-21}	6×10^{-22}
$x_{IP} = 0, x'_{IP} = -1.5$	60	4×10^{-14}	3×10^{-15}
$x_{IP} = 0, x'_{IP} = -1.5$	90	2×10^{-9}	2×10^{-10}
$x_{IP} = 0, x'_{IP} = -1.5$	120	6×10^{-8}	7×10^{-9}
$x_{IP} = 0, x'_{IP} = -1.5$	150	3×10^{-9}	3×10^{-10}
$y'_{IP} = -1$	30	2×10^{-31}	8×10^{-33}
$y'_{IP} = -1$	60	5×10^{-25}	3×10^{-26}
$y'_{IP} = -1$	90	6×10^{-10}	5×10^{-11}
$y'_{IP} = -1$	120	1×10^{-12}	9×10^{-13}
$y'_{IP} = -1$	150	4×10^{-26}	4×10^{-27}
$y'_{IP} = +1$	30	2×10^{-33}	3×10^{-34}
$y'_{IP} = +1$	60	4×10^{-23}	2×10^{-24}
$y'_{IP} = +1$	90	2×10^{-9}	1×10^{-10}
$y'_{IP} = +1$	120	3×10^{-11}	3×10^{-12}
$y'_{IP} = +1$	150	4×10^{-26}	4×10^{-27}
New lattice	30	7×10^{-32}	5×10^{-33}
New lattice	60	1×10^{-29}	3×10^{-30}
New lattice	90	4×10^{-11}	4×10^{-12}
New lattice	120	5×10^{-13}	4×10^{-14}
New lattice	150	6×10^{-27}	6×10^{-28}

Table 1: Power absorbed by the primary mirrors at various azimuthal locations. Nominal beam conditions are discussed in the text. Changes in beam optics are listed in the first column. The two power columns are the radial and tangential polarization components for the power within the acceptance of the optical system.

Three features emerge from Table 1, regardless of beam conditions.

- There is a strong dependence of the power on the azimuth.
- There is a low background region in the vicinity of the 60 degrees counter. Other regions are clearly unsuitable for beamstrahlung detection.
- The background is strongly polarized ($\approx 90\%$)

Figure 5 show signal and background for $0.9 < \lambda < 1.0\mu\text{m}$, for the counter at 72.5 degrees (the 50 degrees counter produces an almost identical plot). Figure 5 has excellent features. At 5.6 meters, the beam pipe is seen at an effective angle of about 11 mrad, and the signal/noise there is large. The signal does not change much when beam conditions change around $\theta = 11\text{mrad}$. In turn, this limits the dynamic range requirements for our counters. The signal exceeds the background well to the left and to the right of $\theta = 11\text{mrad}$, making the signal/noise nearly independent of beam conditions. At the nominal CESR conditions one gets a flux of 5×10^7 photons per counter per second, or 3 per collision.

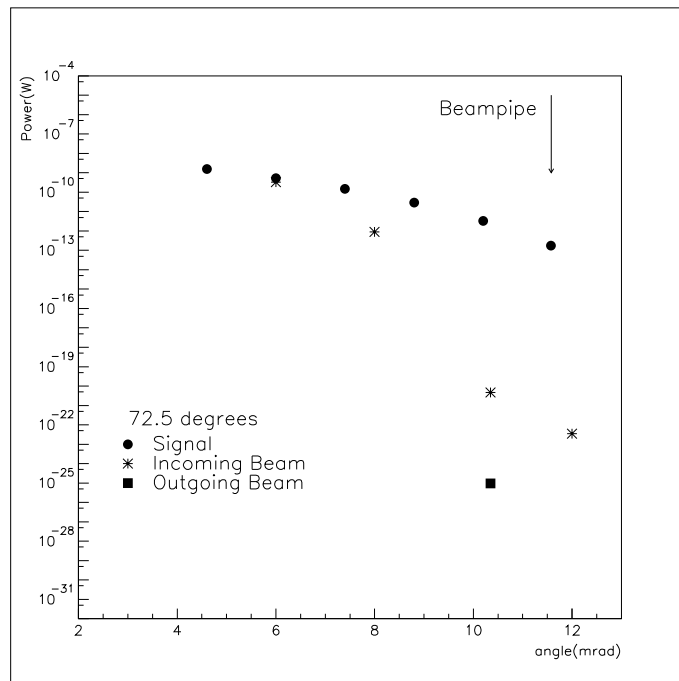


Figure 5: Power versus angle in the infrared region, for a mirror located at 72.5 degrees. Black dots: beamstrahlung power. Stars: incoming beam. White triangles: outgoing beam.

The following points underline the validity of our simulation. The background estimate does not depend appreciably on the synchrotron radiation model used. The two models are extreme in their assumptions about the angular dependence of the Fourier transform,

effectively placing limits on the true value of the background. The background comes predominantly from particles that point to the vicinity of the counter. The two models tend to be in rough agreement at low and medium angle. The background comes principally from the medium beam tails ($2 - 7\sigma$) which are well understood. The background is still much smaller than the signal when the beams angles and positions are changed. The background is still much smaller than the signal when the lattice is changed.

4.2 Other sources of background.

In the following we assume that our optical system, and in particular the primary mirrors, are of laser-optics quality, and that only the backgrounds entering the detector within the optical acceptance will contribute. This corresponds to an effective solid angle efficiency of about 10^{-7} for isotropic radiation. The mirrors image long ribbons of beam pipe on the other side of the interaction region, opposite in azimuth, centered around 5.6 meters, 60 centimeters long and 1.12 centimeters wide. These strips are called in the following the “field-of-view” (FOV). The East detector insertion sees the West detector insertion when properly aligned, a fact we use to establish the delicate alignment.

A particular concern is radiation striking the mirrors or the FOV. Backgrounds striking the FOV must be very small. Due to the geometry of the CESR beam pipe, Fig. 4, the FOV is sheltered against incoming radiation and can be illuminated directly only by radiation originating on the last meter of the orbit with a radiating angle of at least 40 mrad. Clearly the FOV will be illuminated directly in a negligible way.

More relevant is the radiation, generated upstream, that scatters against the beam pipe in the last meter before the funnel, Fig. 4, then scatters in the FOV while aligning itself with the telescope’s acceptance. For the first scattering, the incident angle is of order 1 mrad and the reflecting angle about 40 mrad. For the second scattering, the incident angle is about 40 mrad, and the reflecting angle is 11 mrad. Between the two scattering, the infrared photon direction must be rotated in ϕ by about 60 degrees. A simple mathematical modeling of the beam pipe roughness suggests that this background would be small. The long wavelength and low angles help make the beam pipe a near-perfect mirror. In the limit in which the beam pipe is a perfect mirror, the rescattered backgrounds are zero.

The chosen location is one of the least irradiated regions of CESR. The location is completely sheltered against the hard bend sweeps. The soft bend synchrotron sweep from the incoming beam deposits about one Watt per centimeter. About 10^{-5} of the total radiation is in the infrared frequency window chosen. The mirrors inner edges are located at 4.2 and 5.0 centimeters above the horizontal plane, and are not hit directly by the sweep. A negligible amount of the sweep has the right angle for our detector.

Reference [5] discusses in detail four sources of luminous backgrounds:

1. black-body thermal background;
2. Thompson scattering on the beam pipe electrons;
3. Cherenkov light in the vacuum window;
4. fluorescence in the beam pipe.

These sources were all found to be negligible. Infrared light produces lower backgrounds for all other sources except thermal noise, compared to visible light. Thompson scattering stays the same.

4.3 Detector design.

The beamstrahlung optics starts with two mirrors located in the lower half of the beam pipe, at -50 and -72.5 degrees with respect to the x -axis, 5.6 meters away from the IP (Fig. 6). The mirrors are rectangular, with sides of 7 and 9 millimeters, and they reflect light straight up through vacuum windows of diameter 5.6 millimeters.

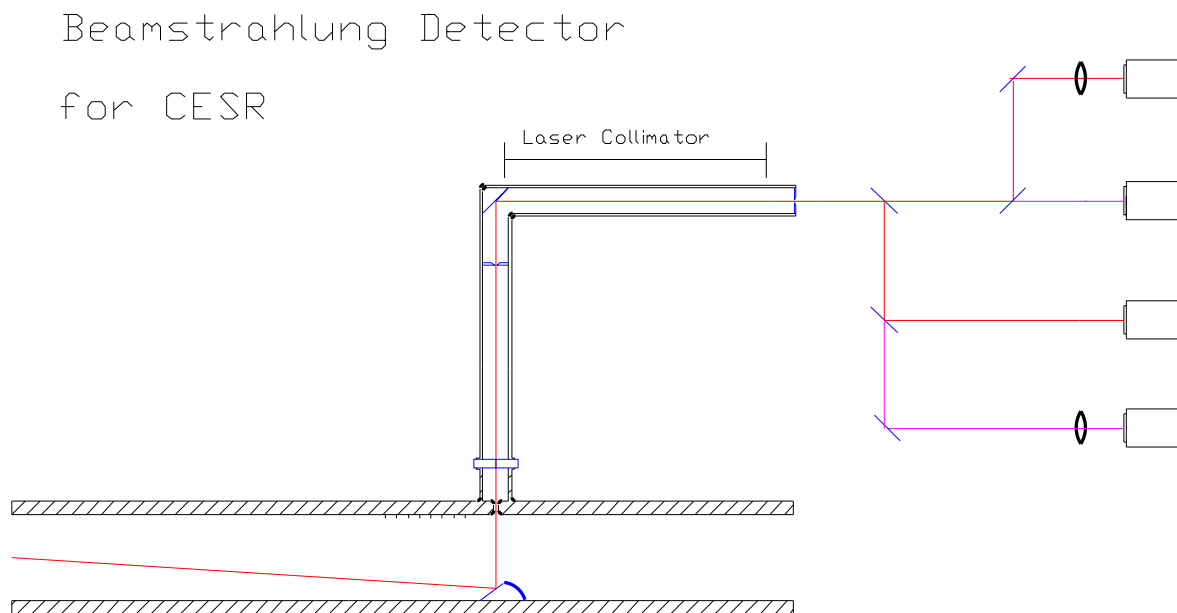


Figure 6: Preliminary design of the beamstrahlung detector. Shown are the primary mirror, vacuum window, two collimators, and four optical channels corresponding to the two polarizations and two frequency windows described in the text.

Light travels up for 60 centimeters, before being collimated to obtain only the component between 10.4 and 11.4 mrad, and then is reflected back to its original direction to recover full polarization information (also, the collimator would lay directly above a large magnet, which is the mechanical support).

A calcite cube splitter can efficiently separate the two polarization components over a wide spectrum. Each polarized beam is then split into two with partially reflecting mirrors. Of the four beams, two are now used for infrared detection, and two for visible light. The former is separated using filters which transmit only above 0.9 microns for the last reflection.

The latter needs no filtering as “normal” photomultipliers (PMT) cut off efficiently at 700 nm. There are four PMTs per viewport (two IR PMTs for signal, two “normal” PMTs for background), and sixteen total in the system.

Optical quality is crucial upstream of the collimator’s iris. The primary mirror will be constructed of a solid piece of aluminum, diamond-machined to $\lambda/20$ flatness. The mirror is slightly larger than the vacuum window to stop stray reflections from the mirror edge. It is heated by a few Watts of RF power, and the monolithic construction helps with thermal stability and cooling. The vacuum window and secondary mirror present no particular problems. All windows materials are fully transparent below one micron, and the secondary mirror could in principle be made exactly as the primary mirror.

The collimator is a simple, two-lenses, one-iris telescope (the total cost, for four collimators, see quote enclosed, is 58,000 dollars). There is no need for precision optics past the iris, because the PMT photocathodes are much larger than the beam spot size. The collimator is about 1.75 meters long and is diffraction-limited. The first lens will need appropriate infrared coating and may have to be custom-made. We realize that because of this the collimator might be less efficient in the visible (which measures backgrounds) than in the infrared.

The collimator iris (in the form of two moveable, expandable slits) is the only moveable part in the system. It is impossible to align such a device, specially considering that it is supported off a magnet. Alignment and stepping motor calibration will be obtained by making use of the FOV on the other side of the IP. By shining a diffuse light from the opposite vacuum windows, and from special small “calibration windows” opposite in azimuth to our mirrors, the location of the IP, and the stepping motor calibration, can be measured directly.

Photomultipliers are the detector of choice. The average number of photoelectrons per beam crossing is less than one, and high gain is needed for pulse-by-pulse studies. Fast-timing information is also needed for pulse-by-pulse studies, and to reject out-of-time backgrounds due to multiple reflections or wrong-beam source. To the best of our knowledge, no hybrid photodiode or other solid-state device was found on the market that could match our needs as well as a PMT.

Hamamatsu has several infrared PMTs. We chose the R-3310-02 PMTs, sensitive down to $1\mu\text{m}$ wavelength. They cost \$3839.09 per unit, for a total (we need eight, plus one spare) of \$34552. Photomultipliers efficient down to $1.4\mu\text{m}$ (R-5509-42) were deemed too expensive (more than 20,000 dollars per unit). They also would have needed cooling to shield against thermal backgrounds.

Photomultipliers can be calibrated on a run-by-run basis by utilizing the last operator step before beam collisions, where the two beams, separated by tens of microns in y , are brought together. The resulting beamstrahlung “seagull” plot [1, 2, 11, 18] provides the calibration needed. Fast-gating electronics and data acquisition complete the hardware. Standard CAMAC devices will be acquired and implemented.

With the viewports and frequency windows described above, one obtains a signal of 3×10^5 photoelectrons per second for the phototubes looking at infrared light, and a much smaller one for the phototubes looking at visible light. The total current for each infrared phototube is 10 nA. A 1% measurement of a single bunch in one of the beams will take approximately 1.5 seconds.

5 Impact of infrastructure Project.

The project will deliver extra luminosity at CESR and at other high-luminosity e^+e^- colliders, both directly, by optimizing beam collision conditions, and indirectly, by helping study the beam-beam limit in more detail. Extra luminosity will result in smaller errors in the crucial CP-violating measurements these colliders are meant to study, and will extend the physics reach of the facility.

Our group is a leader in involving women and minorities in physics. For example our REU site [20] has had, over the last two years, 63% women, 50% minorities, and 56% “first generation” participants (students who are the first in their family to attend college). We have been particularly effective in bringing disadvantaged students in contact with the advanced and nationally prominent physics environment of the Laboratory of Nuclear Sciences at Cornell. Undergraduates have been involved in beamstrahlung work already twice, in both cases producing a publication [2, 5]. We will continue to do so over the foreseeable future. For example, this summer we will be able to bring three African-American physics students to Cornell (so far most minority students were from various engineering disciplines). All plan to attend graduate school, and two have expressed interest in graduating with our group.

The beamstrahlung project is terrific for the scientific development of junior scientists. Here is a project of substantial impact, which can be thoroughly understood with knowledge of electrodynamics, and whose data depend on a variety of effects, which require substantial scientific acumen to disentangle. Yet the whole project is small enough that it can be mastered by a motivated junior scientist.

6 Project and Management Plans.

Professor Bonvicini will be in charge of the project, in particular of the overall design of the device, and procurement of parts. The postdoc will be located at Cornell and will be primarily responsible for working on the interface between the hardware and CESR control system and developing the beamstrahlung monitor operation, monitoring and feedback software. The whole group (WSU, McGill, and Parma) will be available at turn-on. Once the detector is in place the postdoc is expected to lead a program of machine studies to commission the system.

Over the spring we will design and machine the primary mirrors, the vacuum window, and their respective vacuum components. They will be added to the CESR ring in July, during the CESR Shutdown, when vacuum will be broken.

Fabrication of the optics components and electronics assembly will start as soon as the postdoc is hired. McGill University will characterize the photomultipliers, including linearity, gain, stability over time and uniformity of response across the photocathode. Target date for first observation of light, using precision collimation, is February 2001. The full detector should be ready by April 2001. University of Parma will be in charge of all the theoretical calculations needed to compare against the data.

The detector as designed needs no maintenance or management, except for re-alignment when the beams move inside of CESR. Once this task is automated, the detector will need no maintenance.

References

- [1] G. Bonvicini and J. Welch, Nucl. Inst. and Meth. 418, 223, 1998.
- [2] G. Bonvicini, D. Cinabro and E. Luckwald, Phys. Rev. E 59: 4584, 1999.
- [3] G. Bonvicini, CBN-98-12.
- [4] G. Sun, CBN-98-13.
- [5] N. Detgen *et al.*, CBN-99-26.
- [6] For a recent review see “Beam-Generated Detector Backgrounds at CESR”, S. Henderson and D. Cinabro, in *Workshop on High Luminosity e^+e^- Colliders*, Japan (1999).
- [7] “Observation of the dynamic beta effect at the Cornell Electron-Positron Storage Ring with the CLEO detector”, D. Cinabro *et al.*, *Phys. Rev. E* 57, (1998): 1193.
- [8] K. Korbiak, “Observation of dynamical emittance”, <http://motor1.physics.wayne.edu/cinabro/cinabro/education/wsucure/1999wsucure.html>
- [9] R. Coisson, Phys. Rev. A 20, 524, 1979.
- [10] . Bossart *et al.*, Nucl.Instrum.Meth.164:375-380,1979.
- [11] M. Bassetti *et al.*, IEEE Trans.Nucl.Sci.30:2182-2184,1983.
- [12] G. Bonvicini *et al.*, SLAC-PUB-3978, 1985.
- [13] E.G. Bessonov *et al.*, DESY-M-96-08, Apr 1996. 7pp.
- [14] J. Bosser *et al.*, IEEE Trans.Nucl.Sci.30:2164-2166,1983
- [15] D.P. Barber *et al.*, Nucl.Instr.Methods, A338 166, 1994.
- [16] D. Sagan, J. Sikora and S. Henderson, CBN-97-13.
- [17] P. Bambade, SLAC-CN-303, 1985; P. Bambade *et al.*, Phys. Rev. Lett. 62: 2949, 1989.
- [18] G. Bonvicini *et al.*, Phys. Rev. Lett. 62: 2381, 1989.
- [19] G. Bonvicini *et al.*, Nucl. Instr. and Meth. 277, 297, 1989.
- [20] <http://motor1.physics.wayne.edu/cinabro/cinabro/education/wsucure/wsucure.html>
- [21] J. D. Jackson, “Classical Electrodynamics”, Chapter 14, Wiley.